Kinetic model of induced codeposition of Ni-Mo alloys

ZENG, Yue*,[a](曾跃) MA, Ming[a](马铭) XIAO, Xiao-Ming[a](肖小明)
LI, Ze-Lin[a](李则林) LIAN, Shi-Xun[a](廉世勋) ZHOU, Shao-Min[b](周绍民)
[a] *Department of Chemistry, Hunan Normal University, Changsha, Hunan 410006, China*
[b] *Department of Chemistry, Xiamen University, Xiamen, Fujian 361005, China*

The kinetic model of induced codeposition of nickel-molybdenum alloys from ammoniun citrate solution was studied on rotating disk electrodes to predict the behavior of the electrodeposition. The molybdate (MoO_4^{2-}) could be firstly electrochemically reduced to MoO_2, and subsequently undergoes a chemical reduction with atomic hydrogen previously adsorbed on the inducing metal nickel to form molybdenum in alloys. The kinetic equations were derived, and the kinetic parameters were obtained from a comparison of experimental results and the kinetic equations. The electrochemical rate constants for discharge of nickel, molybdenum and water could been expressed as $k_1(E) = 1.23 \times 10^{-9} C_{Ni} \exp(-0.198FE/RT)$ mol/(dm^2·s), $k_2(E) = 3.28 \times 10^{-10} C_{Mo} \exp(-0.208FE/RT)$ mol/(dm^2·s) and $k_3(E) = 1.27 \times 10^{-6} \exp(-0.062FE/RT)$ mol/(dm^2·s), where C_{Ni} and C_{Mo} are the concentrations of the nickel ion and molybdate, respectively, and E is the applied potential vs. saturated calomel electrode (SCE). The codeposition process could be well simulated by this model.

Keywords Kinetic model, induced codeposition, Ni-Mo alloy

Introduction

Owing to the high corrosion resistance, high wearing resistance[1,2] and low hydrogen evolution overpotential[3,4] of Ni-Mo alloys, many investigations have been devoted to the deposition of these deposits. However the codeposition mechanism of Ni-Mo alloys is still not elucidated. Indeed the high overpotential deposition of Mo on Mo, together with the low overpotential of hydrogen evolution on Mo, prevents the deposition of Mo in a pure state. But molybdenum readily codeposites with iron-group metals from aqueous solution. Several hypotheses have been proposed for the codeposition mechanism of Ni-Mo alloys.[5-16] The most investigation mentioned the possible multi-step reduction of some molybdic species. However the type and the further reduction of intermediate molybdenum species are still not well understood. Some authors[5-7] proposed that complexed Ni-Mo species as intermediate are present in the electrolyte. Codeposition of Mo, according to this view, is due to the reduction of a dissolved Ni-Mo complex. This mechanism has been criticized[8,9] because it has not been possible to detect complexed Ni-Mo species in the electrolytes used for codeposition. And other authors[10-13] proposed that the molybdate is firstly electrochemically reduced to molybdenum oxide, for example MoO_2, subsequently undergoes a chemical reduction with atomic hydrogen previously adsorbed on the inducing metal nickel to form molybdenum in alloys. Recently, a new surface-adsorbed intermediate mechanism has been suggested by Podlaha *et al.*,[14-16] in which the induced codeposition of molybdenum with the iron group element occurs with the help of a surface-adsorbed intermediate, $[M(II)\text{-}LMoO_2]_{ads}$, where M represents either Ni, Co or Fe and L is ligand. However, very recently the induced codeposition of molybdenum with iron was investigated using *in situ* surface enhanced Raman spectroscopy (SERS) technique.[17] The results showed that the main species on the electrode surface is a "molybdenum blue" compound as an induced-codeposited intermediate in the electrodeposition of the alloys. Unfortunately, the intermediate existing as $[M(II)LMoO_2]$ was not be detected. A more quantitative approach is therefore needed in order to reach a better understanding of the codeposition mechanism.

In the present paper the mechanism, which has been studied in our previous paper,[13] was employed to

Received February 1, 1999; accepted June 21, 1999.

simulate the codeposition process of Ni-Mo alloys. The kinetic equations were derived, and the kinetic parameters were obtained from a comparison of experimental results and the kinetic equations. The partial currents of Ni, Mo and hydrogen evolution were calculated as a function of different operating parameters. The partial currents thus determined the alloy composition and current efficiency which are compared to experimental results.

Experimental

The experiment of steady state polarization curve was carried out using the computer electrochemical test system (Model ETS ver. 2.0, Tianjin, China), and the working electrode was a Cu rotating - disc electrode of 0.357 cm diameter. The electrode potential was measured in relation to a saturated calomel electrode (SCE). A large platinum gauze served as an auxiliary electrode. Ni-Mo alloys were potentiostatically electrodeposited from ammonium citrate solution containing 0.15 mol/L $NiSO_4$ + 0.10 (Mo) mol/L $(NH_4)_6Mo_7O_{24}$ + 0.3 mol/L $Na_3(C_6H_5O_7)$ + 0.3 mol/L NaCl + 0.45 mol/L $NH_3 \cdot H_2O$. This solution was made up from analytical grade purity compounds and twice distilled water. The pH was adjusted with NaOH or H_2SO_4 to 9.0 for which the alloy deposition efficiency is high. The temperature was kept at 30℃. A more detailed description of the experiment has been reported in a previous paper.[13]

The chemical compositions of the alloys were assayed by an Energy Dispersion Spectrometer (EDS, X-650 9VP, Japan).

Mathematical model

The induced codeposition mechanism of Mo with Ni from ammonium citrate solution has been studied in our previous paper.[13] The investigations indicated that the nickel could be electrodeposited independently of molybdenum. Erust *et al.*[18] indicated that nickel ion complexes strongly with both citrate and ammonia to form multiligand coordination, $[NiCit(NH_3)_m]^-$, in the ammoniun citrate solution, where m, being coordination number of ammonia, is among 0 and 3. Since ammonia and citrate were excess in the baths, nickel ions exist mainly as $[NiCit(NH_3)_3]^-$. Therefore, the electrodeposition of nicel could be expressed as

$$[NiCit(NH_3)_3]^- + 2e \xrightarrow[\text{rds}]{k_1} Ni + Cit^{3-} + 3NH_3 \quad (1)$$

In the induced codeposition of Mo with Ni, the molybdate (mainly existed as MoO_4^{2-} in alkaline solution)[19] is electrochemically reduced to MoO_2, subsequently undergoes a chemical reaction with atomic hydrogen previously adsorbed on the inducing metal nickel to form molybdenum in alloys. Thus it can be predicted that the existence of the surface-adsorbed hydrogen in atomic state affects greatly the deposition of molybdenum.[20] The accepted mechanism of the hydrogen evolution reaction on Ni-base alloys wasstudied by Lasia *et al.*[21-25] They deduced, in all cases, that this reaction proceeded through two steps, the first step is the discharge of water to form atomic hydrogen adsorbed at electrode, and the second step is an electrochemical deadsorption to give off hydrogen, *i.e.*

$$MoO_4^{2-} + 2H_2O + 2e \xrightarrow[\text{red}]{k_2} MoO_2(M)_{ads} + 4OH^- \quad (2)$$

$$H_2O + e \xrightarrow[\text{red}]{k_3} H(M)_{ads} + OH^- \quad (3)$$

$$MoO_2(M)_{ads} + 4H(Ni)_{ads} \xrightarrow{k_4} Mo(Ni) + 2H_2O \quad (4)$$

The side reaction in electrodeposition is hydrogen evolution, that is

$$H(M)_{ads} + H_2O + e \xrightarrow{k_5} H_2\uparrow + OH^- \quad (5)$$

where M represents Ni, Mo or substrate atoms on the surface of electrode. k_1, k_2, k_3 and k_5 in Eq. (1), Eq. (2), Eq. (3) and Eq. (5) are the electrochemical rate constants, respectively.

At the range of high cathode polarization, the current density of the rotating disk electrode for an electrochemical reaction j could be expressed as[26]

$$\frac{1}{i_j} = \frac{1}{i_{D,j}} + \frac{1}{i_{E,j}} \quad \text{or} \quad i_j = \frac{i_{E,j}}{1 + i_{E,j}/i_{D,j}} \quad (6)$$

and $$i_{E,j} = n_j F k_j \quad (7)$$

$$i_{D,j} = 0.62 n_j F D_j^{2/3} \upsilon^{-1/6} S^{1/2} C_j \quad (8)$$

where $i_{D,j}$ and $i_{E,j}$ are the limiting-diffusion current density and the electrochemical polarization current density, k_j is the electrochemical rate constant in the electrochemical reaction j, C_j and D_j are the bulk concentration and the diffusion coefficient for the diffusion limited species, v is the kinematic viscosity, S is the rotation speed (rad/s) of the electrode, n_j is the transfer number of electrons in the electrochemical reaction j, where $n_1 = n_2 = 2$ and $n_3 = n_5 = 1$ in this case, and F is Faraday's constant, respectively.

For simplification, C_{Ni}, and C_{Mo} represent the concentration of $[NiCit(NH_3)_3]^-$ and MoO_4^{2-}, respectively.

Assume that the variation of concentration of water can be neglected during reaction, therefore, the current densities of the electrochemical reaction are respectively

$$i_{E,1} = n_1 F k_{10} C_{Ni}(1-\theta)\exp(-\alpha_1 n_1 FE/RT) \quad (9)$$

$$i_{E,2} = n_2 F k_{20} C_{Mo}(1-\theta)\exp(-\alpha_2 n_2 FE/RT) \quad (10)$$

$$i_{E,3} = n_3 k_{30}(1-\theta)\exp(-\alpha_3 n_3 FE/RT) \quad (11)$$

$$i_{E,5} = n_5 k_{50}\theta_H(1-\theta)\exp(-\alpha_5 n_5 FE/RT) \quad (12)$$

where k_{10}, k_{20}, k_{30} and k_{50} are the electrochemical rate constants at E (applied potential) = 0, α is cathodic transfer coefficient, R is the gas constant, T is absolute temperature, E is potential referred to a saturated calomel electrode (SCE) and $\theta = \theta_H + \theta_{MoO_2}$, where θ_H and θ_{MoO_2} represent the fractional surface coverage of the adsorbed intermediates, both atomic hydrogen and MoO_2, on the surface of electrode, respectively.

If the reactions (1), (2), and (3) are the rate-determining steps (rds) for the electrodeposition of nickel and molybdenum and for the hydrogen evolution, respectively, the current density equations for the electrodeposition of Ni, Mo and hydrogen evolution according to equations (1)-(12) are

$$i_{Ni} = i_1 = n_1 F r_1 = \frac{n_1 F k_{10} C_{Ni}(1-\theta)\exp(-\alpha_1 n_1 FE/RT)}{1 + n_1 F k_{10} C_{Ni}(1-\theta)\exp(-\alpha_1 n_1 FE/RT)/i_{D,1}} \quad (13)$$

$$i_{Mo} = n_{Mo} F r_2 = \frac{n_{Mo} i_2}{n_2} = \frac{n_{Mo} F k_{20} C_{Mo}(1-\theta)\exp(-\alpha_2 n_2 FE/RT)}{1 + n_2 F k_{20} C_{Mo}(1-\theta)\exp(-\alpha_2 n_2 FE/RT)/i_{D,2}} \quad (14)$$

$$i_{H_2} = n_{H_2} F r_5 = n_{H_2} F(r_3 - 4r_4) = n_{H_2} F(r_3 - 4r_2) = n_{H_2} i_3/n_3 - 4n_{H_2} i_2/n_2 =$$

$$\frac{n_{H_2} F k_{30}(1-\theta)\exp(-\alpha_3 n_3 FE/RT)}{1 + n_3 F k_{30}(1-\theta)\exp(-\alpha_3 n_3 FE/RT)/i_{D,3}} - \frac{4 n_{H_2} F k_{20} C_{Mo}(1-\theta)\exp(-\alpha_2 n_2 FE/RT)}{1 + n_2 F k_{20} C_{Mo}(1-\theta)\exp(-\alpha_2 n_2 FE/RT)/i_{D,2}} \quad (15)$$

where i_{Ni}, and i_{Mo} represent the current density for the electrodeposition of nickel and molybdenum, i_{H_2} represents the current density for the hydrogen evolution, and r represents reaction rate, respectively.

As an approximation the expression of θ_H and θ_{MoO_2} are written as

$$\theta_H = \frac{\dfrac{k_{30}\exp(-\alpha_3 n_3 FE/RT)}{1 + n_3 F k_{30}\exp(-\alpha_3 n_3 FE/RT)/i_{D,3}} - \dfrac{4 k_{20} C_{Mo}\exp(-\alpha_2 n_2 FE/RT)}{1 + n_2 F k_{20} C_{Mo}\exp(-\alpha_2 n_2 FE/RT)/i_{D,2}}}{k_{50}\exp(-\alpha_5 n_5 FE/RT)} \quad (16)$$

$$\theta_{MoO_2} = \frac{n_{Mo} k_{20} C_{Mo}\exp(-\alpha_2 n_2 FE/RT)}{k_{40} Q_H(1 + n_2 F k_{20} C_{Mo}\exp(-\alpha_2 n_2 FE/RT)/i_{D,2}} \quad (17)$$

The value of Q_H in Eq. (17) can be calculated from Eq. (16).

At each applied potential the partial current densities are calculated. The total current density, i_T, is the sum of the partial current densities, i_j.

$$i_T = \sum_j i_j \tag{18}$$

The cathodic current efficiency (C.C.E.) for metal deposition is equal to the sum of partial current densities of nickel, i_{Ni}, and molybdenum, i_{Mo}, divided by the total current density

$$\text{C.C.E.}\% = \frac{i_{Ni} + i_{Mo}}{i_T} \tag{20}$$

The molar fraction of molybdenum, X_{Mo}, in the alloys is calculated from the partial current densities according to Eq. (20)

$$X_{Mo} = \frac{i_{Mo}/n_{Mo}}{i_{Ni}/n_{Ni} + i_{Mo}/n_{Mo}} \tag{20}$$

Results

Model parameters

The values of the nickel, molybdenum, and water reaction have been chosen to fit the partial current densities obtained from the experiment using Sigmaplot for windows software. The kinetic parameters fitted for the model is listed in Table 1.

Table 1 The model parameter list

For Ni		For Mo		For H	
k_{10} (dm/s)	$(1.23 \pm 0.26) \times 10^{-9}$	k_{20} (dm/s)	$(3.28 \pm 1.95) \times 10^{-10}$	k_{30} (mol·dm/s)	$(1.27 \pm 0.21) \times 10^{-6}$
		k_{40} (mol·dm/s)	$(6.25 \pm 0.35) \times 10^{-1}$	k_{50} (mol·dm/s)	$(6.57 \pm 3.95) \times 10^{-3}$
α_1	0.099 ± 0.0006	α_2	0.104 ± 0.0006	α_3	0.062 ± 0.0024
				α_5	0.061 ± 0.0024
n_1	2	n_2	2	n_3	1
		n_{Mo}	2	n_5	1
D_1B (dm^2/s) ($[NiCit(NH_3)_3]^-$)	$(7.76 \pm 0.12) \times 10^{-7}$	D_2 (dm^2/s) (MoO_4^-)	$(3.63 \pm 0.64) \times 10^{-7}$	n_{H_2}	2

Influence of applied potential

Fig. 1 shows the experimental and predicted partial current densities of nickel, molybdenum and the hydrogen evolution at different potential. At the potential more positive than -1.2 V, the current efficiency of alloy deposition is very low. Hydrogen evolution is observed, as in the case of pure citrate or molybdate/citrate solutions . In the intermediatepolarization range , between -1.3 V and -1.7 V, the partial current for hydrogen

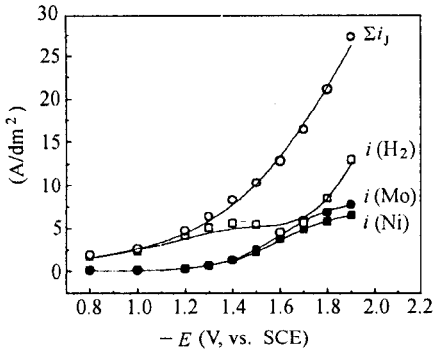

Fig. 1 Experimental (○,□,● and ■) and predicted (—) total and partial current densities of nickel, molybdenum and the hydrogen evolution at different potential.

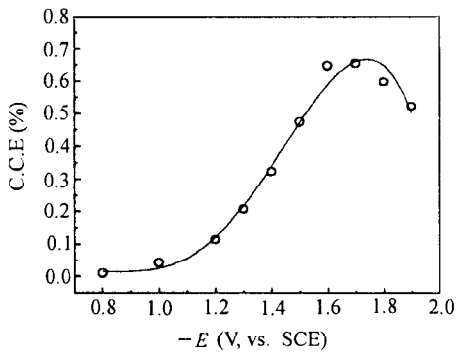

Fig. 2 Comparison between predicted (—) and experimental (○) cathode current efficiency.

evolution is nearly potential independent. At more negative potential, the partial current for hydrogen evolution increases more rapidly than that of nickel and molybdenum discharge, and the current efficiency decreases. The comparison between predicted and experimental cathode current efficiency (C.C.E.) is shown in Fig. 2 . The maximum is obtained at the potential of about -1.7 V.

The measured and calculated contents of molybdenum in alloys are presented in Fig. 3. In low polarization the content of molybdenum in alloys increases with the cathode polarization . In the potential range form -1.6 V to -1.9 V, the partial current increases at the same rate for both nickel and molybdenum, the content of molybdenum remains nearly constant at about 28.5 a/o.

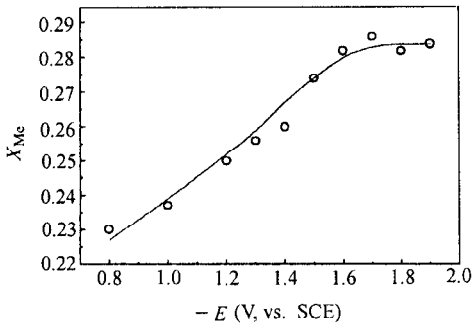

Fig. 3 Predicted (—) and experimental (○) contents of molybdenum in alloys.

Influence of electrode rotation rate on the partial current density of both nickel and molybdenum

According to Eq. (8) the partial limiting-diffusion current densities, $i_{D,2}$, $i_{D,3}$, for nickel and molybdenum are respectively

$$i_{D,1} = 0.62 n_1 F D_1^{2/3} \nu^{-1/6} S^{1/2} C_{Ni} \quad (21)$$

$$i_{D,2} = 0.62 n_2 F D_2^{2/3} \nu^{-1/6} S^{1/2} C_{Mo} \quad (22)$$

Evidently, the plot of the limiting-diffusion current vs. $S^{1/2}$ is a straight line. Fig. 4 shows the relationship between $i_{D,j}$ and $S^{1/2}$ for nickel and molybdenum. The diffusion coefficients were obtained from the slops of the straight line. They are $(7.76 \pm 0.12) \times 10^{-8}$ dm^2/s for $[NiCit(NH_3)_3^-]$ and $(3.63 \pm 0.64) \times 10^{-8}$ dm^2/s for MoO_4^{2-}, respectively.

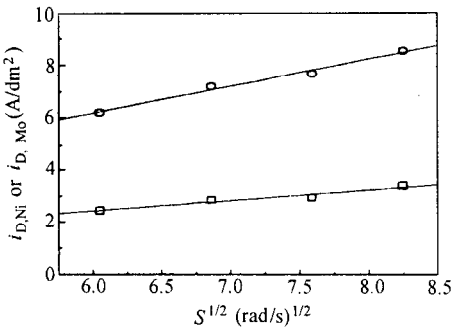

Fig. 4 Relationship between $i_{D,j}$ and $S^{1/2}$ for nickel and molybdenum.

The change of both θ_{MoO_2} and θ_H with applied potential

The variation of coverage of the intermediate species, MoO_2, and H, with applied potential was predicted with Eqs. (16) and (17). As demonstrated in Fig. 5, at the potential more positive than -1.2 V, though the coverage increases for MoO_2, decreases for H with the cathode polarization, this change is small. The mutations appear in intermediate polarization range between -1.2 V and -1.7 V. On the contrary, the coverage decreases for MoO_2 and increases for H with the cathode polarization in the polarization range between -1.7 V and -1.9 V, respectively. At the potential of -1.7 V both valley for H and peak for MoO_2 appear simultaneously. It is at this potential that maximum cathode current efficiency was obtained.

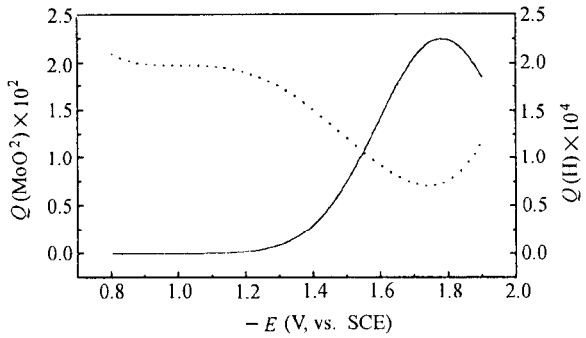

Fig. 5 Variation of coverage of the intermediate species, MoO_2(—) and H (------), with applied potential.

Discussion

The present kinetic model gives a satisfactory de-

scription for the codeposition of the Ni-Mo alloys. At the potential more positive than − 1.20 V the Ni-Mo alloys can not be deposited because the standard electrode potential of reaction (2) is − 1.20 V.[27] At the potential more negative than − 1.2 V, MoO_2 is formed on the surface of electrode. The rates of reactions (1), (2) and (3) increase with the change in potential to more negative. The increase in the rate of reaction (1) results in the increase of the partial current for nickel electrodeposition, the increase in the rate of reactions (2) and (3) results in the increase of the rate of reaction (4). As the rate of reaction (4) increased in analogous rate with the reaction (3), in this polarization range between − 1.3 V and − 1.5 V the partial current for hydrogen evolution (reaction (5)) was roughly constant (see Fig. 1). At the range between − 1.5 V and − 1.6 V the increase in the rate of reaction (2), increasing the coverage of MoO_2, decreasing the coverage of atomic hydrogen, leads to decrease in the partial current for the hydrogen evolution . At potential between − 1.3 V and − 1.6 V, the atomic hydrogen originally being used in the evolution hydrogen (reaction (5)) is partly utilized by reaction (4), which leads to increase in the current efficiency of the electrodeposition. In more negative potential, the increase in the rate of the reaction (3) in relation to both reactions (2) and (4), decreasing the coverage of MoO_2, increasing the coverage of atomic hydrogen, leads to increase in the partial current for the hydrogen evolution, which leads to decrease in the current efficiency of the electrodeposition. These experimental phenomena could be well simulated by this kinetic model.

References

1. Kinh, V. O.; Chassaing, E.; Saurat M., *Electrodeposition Surf. Treat*, **3**, 205(1975).
2. Yao, S. W.; Zeng, Y.; Ge, H. T., *Surf. Tech. (Japan)*, **45**, 643(1994).
3. Zeng, Y.; Yao, S.W.; Ge, H.T., *Plat. Surf. Fin.* (in Chinese), **16**(3), 9(1994).
4. Zeng, Y.; Yao, S.W.; Ge, H.T., *Plat. Surf. Fin.*, **82**(10), 64(1995).
5. Holt, M. L., *Trans. Electrochem. Soc.*, **71**, 301 (1937).
6. Clark, W.P.; Lietzke, M.L., *J. Electrochem. Soc.*, **99**, 245(1952).
7. Vaaler, L.E.; Holt, M.L., *Trans. Electrochem. Soc.*, **88**, 43(1946).
8. Imanaga, H., *J. Chem. Soc., Jap. (Ind. Chem. Section)*, **66**, 1792(1963).
9. Imanaga, H., *J. Chem. Soc. Jap. (Ind. Chem. Section)*, **67**, 286(1964).
10. Fukusima, H.; Akiyama, T.; Akagi, S., *Transaction of the Japan Institute of Metals*, **20**, 358(1979).
11. Ernst, D. W.; Holt, M. L., *J. Electrochem. Soc.*, **105**, 686(1958).
12. Chassaing, E.; Quang, K.V.; Wiart, R., *J. Appl. Electrochem.*, **19**, 839(1989).
13. Zeng, Y.; Yao, S. W.; Ge, H. T., *Acta Phys.-Chim. Sin.* (in Chinese), **11**, 351(1995).
14. Podlaha, E.J.; Landolt, D., *J. Electrochem. Soc.*, **143**, 855(1996).
15. Podlaha, E.J.; Landolt, D., *J. Electrochem. Soc.*, **143**, 893(1996).
16. Podlaha, E.J.; Landolt, D., *J. Electrochem. Soc.*, **143**, 1672(1997).
17. Jiang. Z.; Yao, S. B.; Zhou, S. M., *J. Electroanaly. Chem.*, **445**, 205(1998).
18. Ernst, D. W.; Amlie, R. F.; Holt, M. L., *J. Electrochem. Soc.*, **102**, 461(1955).
19. Honing, D. S.; Kustin, D. M., *Inorg. Chem.*, **11**, 65 (1972).
20. Zeng, Y.; Yao, S. W.; Cao. X. Q.; Huang, H. X.; Zhong, Z. Y.; Ge, H. T., *Chinese J. Chem.*, **15**, 193 (1997).
21. Chen, L.; Lasia, A., *J. Electrochem. Soc.*, **138**, 3321 (1991).
22. Chen, L.; Lasia, A., *J. Electrochem. Soc.*, **139**, 3214 (1992).
23. Chen, L.; Lasia, A., *J. Electrochem. Soc.*, **139**, 3458 (1992).
24. Rami. A.; Lasia, A., *J. Appl. Electrochem.*, **22**, 376 (1992).
25. Los, P.; Rami, A.; Lasia, A., *J. Appl. Electrochem.*, **23**, 135(1993).
26. Greef, R.; Peat, T., *Construmental Methods in Electrochemisty*, Halsted Press, New York, 1985, p.126.
27. Dean, J. A., *Gmelin Handbook, Mo Suppl.* Vol. A2b, Berlin, Springer-Verlag, 1998, p.132.

(JIANG, X.H.; DONG, L.J.)